

Optimal Estimation of Position and Heading for Mobile Robots Using Ultrasonic Beacons and Dead-reckoning

Lindsay Kleeman (MIEEE)

Intelligent Robotics Research Centre
Department of Electrical and Computer Systems Engineering
Monash University, Australia

Abstract

An active beacon localisation system is described that estimates position and heading for a mobile robot. An Iterated Extended Kalman Filter is applied to the beacon and dead-reckoning data to estimate optimal values of position and heading, given a model for the localiser and robot motion. This paper describes the implementation and experimental results of the localisation system. Position and heading angle updates are calculated in real time every 150 milliseconds with a measured standard deviation of path error of 40 mm in a 12 metre square workspace.

1. Introduction

Absolute position and heading angle determination of mobile robots is necessary for long term reliable operation. The effects of wheel slippage and wheel imperfection cause the accumulation of errors in localisers which rely on the integration of wheel rotation increments. This paper solves the problem in an effective and practical manner using active ultrasonic beacons at known positions. Although active beacons are at odds with notions of complete robot autonomy in an unstructured environment, they offer advantages of accuracy, simplicity, speed and cost - factors of interest to industrial and office applications, where the environment can be partially structured. The use of active beacons allows mobile robots to perform adaptive and autonomous activities, such as exploration, online path planning and obstacle avoidance.

The concept of beacon systems for localisation is not new [1, 2, 3, 4]. The system described in this paper is a significant improvement over an earlier version [2] in terms of update speed and accuracy, particularly for moving robot vehicles. The system in this paper takes a different approach to the one in [1] where an *a priori* map of a static environment, containing passive ultrasonic beacons, is assumed which does not require active

beacons. The two approaches are complementary, since a map of the environment can be *established* using the system described here with an appropriate range finder[6]. Other localisation systems use beacons placed at known positions in the environment: [3] uses reflective strips in the environment for a rotating laser mounted on the robot, and [4] uses ultrasonic pulses from the robot with an infrared return from the beacon. The laser system [3], although very precise, is considerably more expensive than the ultrasonic system described here. The beacons in [4] are more complex than the beacons of this paper, since they require infrared coded transmission in addition to reception of ultrasonic pulses from the robot. Reference [4] provides a useful noise rejection approach similar to that employed here.

The ultrasonic localiser of this paper has been developed as part of an autonomous robot project described in [6]. The localiser has been found to be both robust and accurate for moving autonomous robot vehicles. This paper briefly introduces the hardware structure of the system described more fully elsewhere [2, 5] and concentrates on the robust implementation of an Iterated Extended Kalman Filter (IEKF) [11] to optimally estimate the position and heading angle of the mobile robot. The results of validity and accuracy experiments are presented to quantify the performance of the localisation system.

2. Localiser Structure

The components of the localisation system are shown in figure 1. There are six ultrasonic beacons in the 12 metre square laboratory connected to a transmitter controller which sequences the firing of the beacons in a cyclical manner 123456123 etc. Successive beacons are fired 150 msec apart to allow settling of reverberation between pulses. A beacon is *fired* by transmitting a 40 kHz 2.5 msec burst. Beacon 1 is distinguished by transmitting two bursts 3 msec apart, as shown in figure 2. The measured positions and the approximate time between

firing of the beacons are known to the ultrasonic receiver on board the robot vehicle.

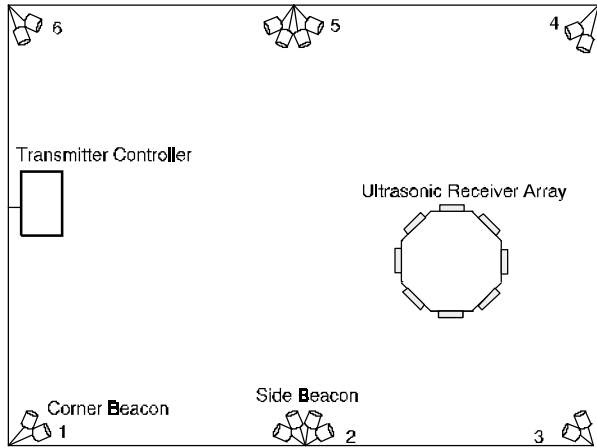


Figure 1 - Overview of Localiser (not to scale).

The receiver array is composed of eight ultrasonic receivers arranged at 45 degree intervals. The receivers are interfaced to a microprocessor that logs arrival times and amplitudes of beacon pulses and passes it onto a Transputer for position and orientation estimation using Kalman filtering. The arrival time accuracy is limited by a 0.6 msec rise time of the pulse envelope, giving a standard deviation of arrival times of 0.2 msec.

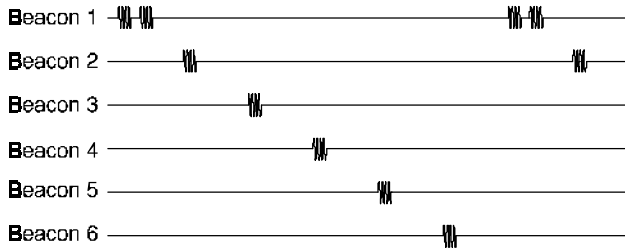


Figure 2 - Sequence of Beacon Firing.

3. System Modelling and Kalman Filtering Equations

A brief review of Kalman filtering [1, 11, 12, 13] is presented in this section using the notation of [11].

3.1. Review of Kalman Filtering

Kalman filtering is an algorithm for optimally estimating the n dimensional state of a system, denoted \mathbf{x} , given a set of measurements in the m dimensional vector \mathbf{y} . The state for our localiser contains the position, orientation and velocity of the robot, as well as state information of the localiser itself, such as the speed of sound and beacon cycle time. The measurements are the arrival times and amplitudes of the received pulses and the dead-reckoning information obtained from the wheel position encoders on the robot.

The localiser is modelled as a discrete time system, where each sample time corresponds to the time of firing of each beacon. Thus the state is updated more than 6 times a second. The Kalman filter problem is formulated in terms of two equations: the *state transition equation*; and the *measurement equation*. In a linear system, this takes the form:

$$\mathbf{x}(k+1) = \Phi \mathbf{x}(k) + \mathbf{w}(k+1) \quad (1)$$

$$\mathbf{y}(k+1) = \mathbf{M} \mathbf{x}(k+1) + \mathbf{v}(k+1) \quad (2)$$

where Φ is called the state transition matrix, and \mathbf{M} is called the measurement matrix, $\mathbf{w}(k+1)$ is state noise and $\mathbf{v}(k)$ is the measurement noise with

$$E[\mathbf{w}(k+1)] = 0, E[\mathbf{w}(k+1) \mathbf{w}(k+1)^T] = \mathbf{Q}(k) \quad (3)$$

$$E[\mathbf{v}(k)] = 0, E[\mathbf{v}(k+1) \mathbf{v}(k+1)^T] = \mathbf{R}(k) \quad (4)$$

where $E[]$ is the expectation, and \mathbf{Q} and \mathbf{R} are diagonal variance matrices of the state and measurement noise. Both \mathbf{Q} and \mathbf{R} are assumed to be known or can be reliably estimated online. The Kalman filter has two steps per measurement cycle: i) state prediction, ii) measurement processing.

3.2. State and Error Prediction

The system modelling in the state transition equation (1) is used to predict the next state. Given the state at time sample k , the state at time $k+1$ called $\hat{\mathbf{x}}(k+1 | k)$ is predicted:

$$\hat{\mathbf{x}}(k+1 | k) = \Phi(k+1, k) \hat{\mathbf{x}}(k | k) \quad (5)$$

The predicted error covariance matrix can also be computed at this stage:

$$\mathbf{P}(k+1 | k) = \Phi(k+1, k) \mathbf{P}(k | k) \Phi^T(k+1, k) + \mathbf{Q}(k) \quad (6)$$

3.3. Measurement Processing

The new measurement or observation $\mathbf{y}(k+1)$ is compared with the predicted measurement, to form the observation error or innovation, $\mathbf{oe}(k+1)$:

$$\mathbf{oe}(k+1) = \mathbf{y}(k+1) - \mathbf{M}(k+1) \hat{\mathbf{x}}(k+1 | k) \quad (7)$$

The predicted state is added to a matrix-scaled value of the innovation, with the matrix scaling factor called the *Kalman gain* $\mathbf{K}(k+1)$:

$$\hat{\mathbf{x}}(k+1 | k) = \hat{\mathbf{x}}(k+1 | k) + \mathbf{K}(k+1) \mathbf{oe}(k+1) \quad (8)$$

where the Kalman gain is given by:

$$\mathbf{K}(k+1) = \mathbf{P}(k+1|k)\mathbf{M}^T(k+1) \cdot \left[\mathbf{M}(k+1)\mathbf{P}(k+1|k)\mathbf{M}^T(k+1) + \mathbf{R}(k+1) \right]^{-1} \quad (9)$$

The new state error covariance matrix is computed by:

$$\begin{aligned} \mathbf{P}(k+1 | k+1) &= [\mathbf{I} - \mathbf{K}(k+1) \mathbf{M}(k+1)] \mathbf{P}(k+1 | k) \quad (10) \\ &= [\mathbf{I} - \mathbf{K}(k+1) \mathbf{M}(k+1)] \mathbf{P}(k+1|k) [\mathbf{I} - \mathbf{K}(k+1) \mathbf{M}(k+1)]^T + \\ &\quad \mathbf{K}(k+1) \mathbf{R}(k+1) \mathbf{K}^T(k+1) \quad (11) \end{aligned}$$

where equation (11) is better numerically conditioned than equation (10) [11, p270].

3.4. Extension to Non-Linear Problems - The Iterated Extended Kalman Filter.

In practice, the state and measurement equations are often non-linear and the state equation takes the form:

$$\mathbf{x}(k+1) = \mathbf{f}(\mathbf{x}(k), \mathbf{u}(k)) + \mathbf{w}(k+1) \quad (12)$$

where $\mathbf{u}(k)$ represents external inputs to the system. The non-linear measurement equation has the form:

$$\mathbf{y}(k+1) = \mathbf{h}(\mathbf{x}(k+1)) + \mathbf{v}(k+1) \quad (13)$$

When the system non-linearity is not "too severe", the system can be linearised about an operating point, and the linear Kalman filter equations applied. The best operating point can be obtained by iteration [11], giving equations known as the **Iterated Extended Kalman Filter (IEKF)**.

3.5. Selection of the State Variables

The state vector should include all variable information necessary to predict the next state of the robot and to enable measurements to be expressed in terms of the state. The robot position, (x_{pos}, y_{pos}) , velocity magnitude, \mathbf{v} , and direction, θ , are incorporated in the state. Also needed is the state of the beacons, such as the beacon cycle time, T , and the speed of sound, s . These parameters are not known precisely *a priori*, and are estimated online. The beacon firing time, t_0 , is incremented when each beacon fires and needs to be present in the state vector, since the measurement equation requires this information. The state vector is:

$$\mathbf{x} = [x_{pos} \ y_{pos} \ v \ \theta \ T \ t_0 \ s]^T \quad (14)$$

3.6. State Transition Equations

The state transition equations (15) below define the function \mathbf{f} in equation (12) for the localisation system.

$$\begin{aligned} x_{pos}(k+1) &= x_{pos}(k) + v(k) T(k) \cos\theta(k) \\ y_{pos}(k+1) &= y_{pos}(k) + v(k) T(k) \sin\theta(k) \\ v(k+1) &= v(k) \\ \theta(k+1) &= \theta(k) + \Delta\theta(k) \\ T(k+1) &= T(k) \\ t_0(k+1) &= t_0(k) + T(k) \\ s(k+1) &= s(k) \end{aligned} \quad (15)$$

The input $\Delta\theta(k)$ is obtained from the dead-reckoning system on board the robot and will be discussed in section 4.5. The linearised state transition matrix Φ is the partial derivative matrix:

$$\Phi = \frac{\partial \mathbf{f}_i}{\partial \mathbf{x}_j} = \begin{bmatrix} 1 & 0 & T \cos\theta & -T v \sin\theta & v \cos\theta & 0 & 0 \\ 0 & 1 & T \sin\theta & T v \cos\theta & v \sin\theta & 0 & 0 \\ 0 & 0 & 1 & 0 & 0 & 0 & 0 \\ 0 & 0 & 0 & 1 & 0 & 0 & 0 \\ 0 & 0 & 0 & 0 & 1 & 0 & 0 \\ 0 & 0 & 0 & 0 & 1 & 1 & 0 \\ 0 & 0 & 0 & 0 & 0 & 0 & 1 \end{bmatrix} \quad (16)$$

3.7. Ultrasonic Measurement Equations

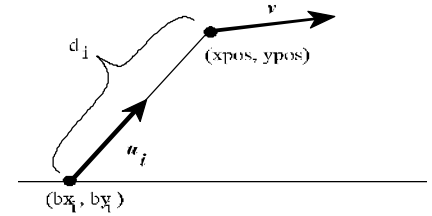


Figure 3 - Measurement Geometry.

In this section, the arrival time of the pulses from the ultrasonic beacons is derived in terms of the state vector \mathbf{x} , which defines the non-linear function \mathbf{h} of equation (13). Here the robot position and velocity are taken into account as well as the state of the ultrasonic beacons. The subscript i is used to denote the beacon number from which the pulse has been sent. The distance from the robot to the beacon is:

$$d_i = \sqrt{(x_{pos} - b_{x_i})^2 + (y_{pos} - b_{y_i})^2} \quad (17)$$

and the unit vector representing the direction from the beacon to the robot is given by:

$$\mathbf{u}_i = \frac{1}{d_i} (x_{pos} - b_{x_i}, y_{pos} - b_{y_i}) \quad (18)$$

The arrival time of the pulse from beacon i is denoted by t_i and is expressed in terms of the firing time t_0 :

$$t_i = t_0 + t_{flight} \quad (19)$$

where t_{flight} is the time of flight of the ultrasonic pulse to the new robot position at time t_i . Assuming the robot speed and direction remain constant during t_{flight}

$$t_{flight} = \frac{d_i + t_{flight} v(\cos\theta, \sin\theta) \cdot \mathbf{u}_i}{s} \quad (20)$$

solving for t_{flight} and substituting in equation (19)

$$t_i = t_0 + \frac{d_i}{s - v(\cos\theta, \sin\theta) \cdot \mathbf{u}_i} = \mathbf{h}_i(\mathbf{x}) \quad (21)$$

Equation (21) forms the measurement equation (13). As pulses are received the measurement equation (21) changes due to incrementing i modulo the number of beacons. Each measurement is treated independently and hence the measurement vector is one dimensional. Differentiating equation (21) gives the linearised measurement matrix \mathbf{M} :

$$\mathbf{M} = \begin{bmatrix} \beta_{t_i} & \beta_{t_i} \\ \beta_{x_{pos}} & \beta_{y_{pos}} & \beta_v & \beta_\theta & \beta_T & \beta_{t_0} & \beta_s \end{bmatrix}^T \quad (22)$$

A closed form solution for each component can be obtained [7], for example:

$$\frac{\beta_{t_i}}{\beta_{x_{pos}}} = \frac{u_{ix} + \frac{v \cdot (1 - u_{ix}^2 - u_{iy}^2)}{d_i (s - v \cdot \mathbf{u}_i)}}{(s - v \cdot \mathbf{u}_i)} \quad (23)$$

where $\mathbf{u}_i = (u_{ix}, u_{iy})$ and $v = v(\cos\theta, \sin\theta)$.

3.8. Incorporation of Dead Reckoning Data

The dead-reckoning data is read in the *incremental* form of robot angular velocity and robot speed, so that the effects of drift are minimised. The dead-reckoning measurements are only accurate over short distances, and accumulate error due to wheel slippage and deformation. This contrasts with the ultrasonic beacon measurements, which have random independent errors that do not accumulate but are not smooth. Thus the two measurements complement each other.

The angular velocity data from dead-reckoning cannot be expressed in terms of the state. A more efficient approach is to define an *input* to the state transition equation for \mathbf{q} :

$$\theta(k+1) = \theta(k) + \Delta\theta(k) = \theta(k) + T(k) \omega(k) \quad (24)$$

where $\mathbf{w}(k)$ is the angular velocity at time step k . The speed of the robot is treated as a measurement since it is a direct function of the state:

$$\text{speed}(k+1) = v(k+1) \quad (25)$$

3.9. Rejecting Echoed Arrival Times

The pulse arrival time of an ultrasonic beacon is sometimes delayed due to an indirect path incorporating reflections off obstacles, walls, ceiling or floor. This may occur when the direct path is obscured. These delayed pulses will be referred to as *echoed arrival times*.

An echoed arrival time should be identified and rejected, otherwise the IEKF will produce a grossly erroneous state estimate or even diverge. During initialisation of the IEKF, all arrival times are assumed to have a high variance. This prevents echoed arrival times causing divergence of the IEKF, but slows initial convergence of the state.

Once the IEKF has converged sufficiently, echoed arrival times can be identified from the observation error in equation (7). If the observation error is an outlier statistically, the measurement is rejected.

3.10. State Transition Noise Variances.

The state transition variance matrix, \mathbf{Q} in equation (3), is assigned based on the robot motion type available online from the path planner. Four categories are used: stationary, no acceleration, straight ramp and curve. The incorporation of the dead-reckoning heading information as an input sets the heading variance to the square of an offset plus a fraction of the angle increment \mathbf{Dq} of equation (24).

3.11. Measurement Noise Variances.

The variance of errors in pulse arrival times is needed by the IEKF (\mathbf{R} matrix). A simple constant has been employed to model the measurement noise variance. More complicated models have been suggested in [4] whereby the standard deviation is a linear function of distance plus an offset, to compensate for the inaccurate estimation of the speed of sound in [4]. These models are not adopted here since the speed of sound is estimated online.

The arrival time error variance was determined experimentally by examining the observation error from data received when the robot vehicle was stationary. The standard deviation was found to be approximately 0.2 msec and reasonably independent of robot position and beacon identity.

4. Experimental Results and Performance of the System

The localiser is mounted above the centre of the driving wheel base of the Robuter mobile robot vehicle. The paths taken by the robot vehicle during several test runs were recorded on the floor using a pen attached to the driving wheel base. The drawn paths were digitised at approximately 50 points per path by measuring the x and y coordinates on the laboratory with estimated accuracy of 10 mm. The raw arrival times and receiver amplitudes from the ultrasonic beacons and Robuter motion data were stored in a data file. The IEKF was run with the raw data and the minimum signed difference (positive to the left) between localiser and measured path was evaluated and is referred to as the *path error*.

Figure 4 shows the path taken by the Robuter. The localiser path refers to the results of the IEKF process with beacon, robot motion control and dead-reckoning data inputs. The times at corners are indicated for reference purposes. The IEKF is given 15 seconds in the initialisation phase and converges to the correct position at 20 secs. There is an offset in the first straight from $t=35$ to 51 due to further fine tuning of the IEKF state, but after this the localiser path accurately follows the robot's true path. On corners the localiser path is on the outside.

The path error is plotted in figure 5. The major excursions occur on corners after the initial straight. The maximum error is limited to 100 mm, with a standard deviation in path error from 20 seconds until 120 seconds of 40 mm.

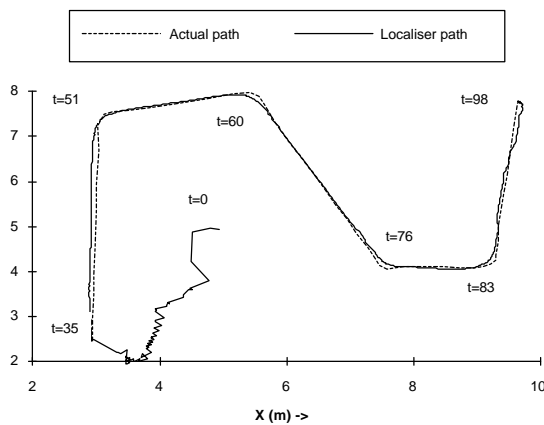


Figure 4 - Actual Path and Localiser Path.

The heading angle of the path and localiser are plotted in figure 6. The localiser performs less accurately on corners. The reason for the path error and the heading error on corners is apparent from figure 6 where ringing in the actual heading angle of the PID controller of the Robuter wheel locomotion is evident at the start and end of corner movements. The dead-reckoning information

used by the IEKF is the path *commanded*, not the actual wheel increments which could not be easily accessed. Evidently the Robuter PID controller needs tuning. Ideally the wheel increments should be read directly.

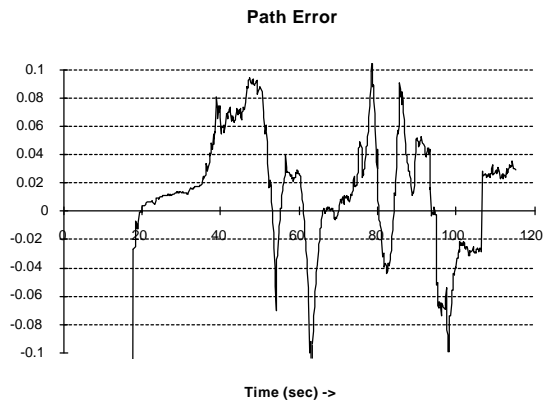


Figure 5 - Path Error of Experimental Data.

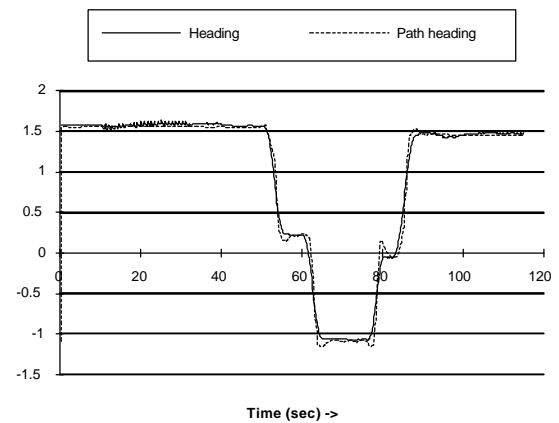


Figure 6 - Actual Heading and Localiser Heading.

The observation errors in figure 7 indicate echoed arrival times. Those above 3 msec are rejected by the localiser. There are a few just below this threshold which cause corresponding path errors in figure 5.

The capability of the localiser to estimate the speed of sound is shown in figure 8, where three different initial estimates of the speed of sound were set, and all converge on the same value in the end. All initial standard deviations were set at 5 m/sec.

Since it was discovered that the dead-reckoning data is unreliable when the Robuter overshoots on corners, results were analysed without this data [7]. The path error standard deviation was 35 mm and actually *less* than that with dead-reckoning measurements. However, the *position* error along the path (not measured) is strongly suspected to be worse due to the noisier speed estimate (not shown). Also, the path error and heading estimates were not as smooth.

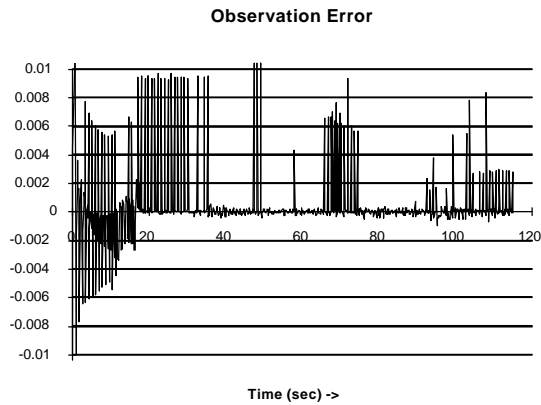


Figure 7 - Observation Errors

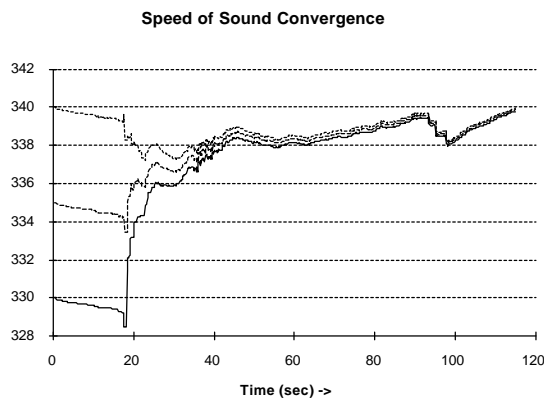


Figure 8 - The Speed of Sound Convergence.

5. Conclusions

A localisation system has been presented which successfully integrates both ultrasonic beacon data with dead-reckoning data in a working mobile robot system. Experimental verification of the system has been performed. The use of the Iterated Extended Kalman Filter in real time proved effective for not only estimating the position and heading, but also rejecting echoed arrival data and providing an estimate of the uncertainty in the localiser output.

6. Acknowledgements

Thanks are expressed to Jeff Dun and John Badcock who wrote the transputer communication routines in the localiser, and Shaun Geddes who provided excellent technical assistance. Financial assistance was obtained from the GIRD team lead by Kemal Ajay and Ray Jarvis,

and funded jointly by the Australian Government, BHP and Monash University.

7. References

- [1] J. F. Leonard, H. F. Durrant-Whyte, "Mobile robot localization by tracking geometric beacons", IEEE Transactions Robotics and Automations Vol. 7 No. 3, pp 376-382, June 1991.
- [2] L. Kleeman, "Ultrasonic autonomous robot localisation system", IEEE international conference Intelligent Robots and Systems '89 Tsukuba, JAPAN, pp.212-219 September 1989.
- [3] K. Hyypya, "Lulea turbo turtle (LTT)", IEEE international conference Intelligent Robots and Systems '89 Tsukuba, JAPAN, pp.620-623 September 1989.
- [4] C. Duriev, H. Clergeot and F. Monteil, "Localization of a mobile robot with beacons taking erroneous data into account", IEEE International Conference on Robotics and Automation, Scottsdale AZ, USA, pp.1062-1068, 1989.
- [5] L. Kleeman, "Ultrasonic autonomous robot localisation system," Monash University, Dept. Electrical and Computer Systems Engineering, Technical Report MECSE 89-8, 1989.
- [6] J. Badcock, J. Dun, K. Ajay, L. Kleeman and R. A. Jarvis, "Autonomous robot navigation", Monash University, Dept. Electrical and Computer Systems Engineering, Technical Report MECSE 91-4, 1991.
- [7] L. Kleeman, "Optimal position and velocity estimation of an autonomous robot vehicle using ultrasonic beacons", Technical report MECSE-91-3, Department of Electrical and Computer Systems Engg., Monash University 1991.
- [8] R. A. Jarvis, "An intelligent robots research centre - work in progress," Proceedings of 19th ISIR, International Symposium and Exposition of Robotics, pp. 149-186, Sydney, Australia, Nov. 1988.
- [9] R. A. Jarvis, J. C. Byrne and K. Ajay, "An intelligent autonomous guided vehicle: localisation, environmental modelling and collision free path finding," Proceedings of 19th ISIR, International Symposium and Exposition of Robotics, pp.767-792, Sydney, Australia, Nov. 1988.
- [10] P. K. Chande and P. C. Sharma, "A fully compensated digital ultrasonic sensor for distance measurement," IEEE Trans. on Instrumentation and Measurement, Vol. IM-33, No.2, June 1984, pp.128-129.
- [11] A. H. Jazwinski, *Stochastic Processes and Filtering Theory*, (Mathematics in Science and Engineering, Vol. 64), Academic Press, 1970.
- [12] B. D. O. Anderson and J. B. Moore, *Optimal Filtering*, Prentice-Hall, 1979.
- [13] S. M. Bozic, *Digital and Kalman Filtering*, Edward Arnold, 1979.